Hydrothermal Synthesis And Visible-light Photocatalytic Activity Of SnS_2/TiO_2 Composite Nanoflakes

Jing Li[a,*], Xihua Du[b], Zhiqiang Zhou[c], YanChen[d]

Collgeg of Chemistry and Chemical Engineering, Xuzhou Institute of Technology, Xuzhou 221111, China

[a]lijingxz111@163.com, [b]dxh@xzit.edu.cn, [c]93929136@qq.com, [d]chenyan681110@126.com

Keywords: Composite materials; In-situ synthesis; Photocatalysis; SnS_2/TiO_2

Abstract: SnS_2/TiO_2 composite photocatalysts with high visible-light photocatalytic activity were synthesized via the hydrothermal treated from tin (IV) chloride pentahydrate, citric acid, thioacetamide and commercial P25 TiO_2 at 150 ºC for 12h. Powder X-ray diffraction and transmission electron microscopy revealed that products were bulk-pure hexagonal phase SnS_2 and rutitle-anatase phase TiO_2 nanoflakes. UV-vis diffuse reflectance spectra disclosed that the as-synthesized SnS_2/TiO_2 nanoflakes had optical bandgaps in the range of about 2.32 - 2.41 eV. In addition, the photocatalytic performances of the as synthesized SnS_2-based nanoparticles were evaluated by degrading methyl orange (20 mg/L MO) in deionized water under the visible-light and real sunlight irradiation. The results demonstrated that all the SnS_2 and SnS_2/TiO_2 products had high visible-light photocatalytic activity, and the most efficient photocatalyst was the molar ratios of Ti: Sn is 0.2. The greatly photocatalytic performance of the as-synthesized SnS_2/TiO_2 composite nanoparticles was mainly attributed to the matching band potentials of SnS_2 and TiO_2 and the efficient charge transfer and separation at their tightly integrated interface.

1. Introduction

Semiconductor photocatalytic process has shown a application potential as a low-cost, environmental treatment technology in wastewater industry, and the development of high performance photocatalysts is vital for the application of photocatalysis technique in large-scale wastewater treatment. SnS_2 and TiO_2 are semiconductors with the band gaps of about 2.2 and 3.2 eV, respectively [1-6]. They are the most promising photocatalysts owing to their low cost, innocuity, high photocatalytic activity and good stability [1-6]. Moreover, they have matched band potentials, that is, both the valence band and conduction band potentials of SnS_2 are more negative than those of TiO_2 [1]. This thermodynamically allows the photogenerated electron transfer from the conduction band of SnS_2 to the conduction band of TiO_2 under visible light ($\lambda > 420$ nm) irradiation, which can enhance the separation of photogenerated electrons and holes in SnS_2 and bring about the sensitization of TiO_2 [1]. Thus, the SnS_2/TiO_2 composites with appropriate compositions should have higher visible light-driven photocatalytic activity than individual SnS_2 and TiO_2.

Herein, we report the composition-tunable preparation of SnS_2/TiO_2 nanocomposites via hydrothermal treatment of different amounts of commercial Degussa P25 TiO_2 in the presence of SnS_2 nanoparticles at 150 °C for 12 h. The structures, compositions and optical properties of the as-prepared products are characterized by X-ray diffraction, transmission electron microscopy and UV-Vis diffuse reflectance spectra. The photocatalytic properties of as-synthesized were tested by the degradation of aqueous methyl orange(MO) under visible light ($\lambda > 420$ nm) and sunlight irradiation.

2. Experimental

All the chemical reagents used were analytically pure and purchased directly from Sinopharm Chemical Reagent Co., Ltd.

SnS_2/TiO_2 composite photocatalysts were synthesized via hydrothermal treatment. Firstly, 5 mmol citric acid (HCA) and 10 mmol thioacetamide (TAA) was dissolved in 10 ml of distilled water

respectively. Then the amount of commercial Degussa P25 TiO_2 (according to different molar ratios of Ti: Sn which were 0.08, 0.2, 0.3, 0.5, 1) and $SnCl_4 \cdot 5H_2O$ were added to a beaker and well dispersed with 20ml distilled water, finally HCA aqueous solution and thioacetamide aqueous solution were slowly added to the mixture aqueous solution of Sn^{4+} and P25 TiO_2 with stirring in turn, the reaction solution was maintained at 150 ºC for 12h. The resulting yellowish precipitate were washed with distilled water and absolute ethanol. finally, products were dried in vacuum at 100 ºC for 5h. Herein, in order to facilitate the description the synthesized product, we abbreviated compositematerials as P25-8, P25-20, P25-30, P25-50, P25-100, respectively.

Powder X-ray diffraction (XRD) patterns were recorded on a German Bruker AXS D8 ADVANCE X-ray diffractometer. Transmission electron microscopy (TEM) images were taken on a PhilipsTecnai-12 TEM operated at an accelerating voltage of 120kV. UV–vis diffuse reflectance spectra were obtained on a Japan Shimadzu UV-3101PC UV–vis-near infrared spectrophotometer using $BaSO_4$ as reference.

Photocatalytic properties of as producted nanoflakes were tested in the degradation of 20.0 mg/L MO aqueous under visible-light and real sunlight irradiation. For comparison, the hydrothermal treated commercial Degussa P25 TiO_2 at 150 ºC for 12h was also tested under the same conditions. The photocatalytic reactor includes mainly four parts, an illumination system including an 200W Xe lamp, cut-off filter ($\lambda > 420$ nm) and cooling attachment such as air pump and electric fan, reactor (two-layer Pyrex glass bottles of 400 ml capacity, and the space between two layers is filled by a circulating water to cool the reactor), magnetic stirrer and temperature controller.

3. Results and discussion

Fig. 1 shows the XRD patterns of the products derived from the hydrothermal reaction of 5 mmol $SnCl_4 \cdot 5H_2O$, 5 mmol citric acid (HCA), 10 mmol TAA and appropriate amounts of P25 TiO_2 at 150 ºC for 12h. The bottom characteristic diffraction peaks correspond to hexagonal phase SnS_2 according to the (JCPDS card no. 00-023-0677). (P25-8) ~ (P25-100) can be indexed to SnS_2, rutile and anatase phases TiO_2, and P25 TiO_2 is made up rutitle and anatase TiO_2. The sizes of SnS_2, (P25-8) ~ (P25-100) and P25 TiO_2 were calculated to be about 13 nm, 18 nm, 21 nm, 20 nm, 23 nm and 22 nm using the Debye Scherrer formula.

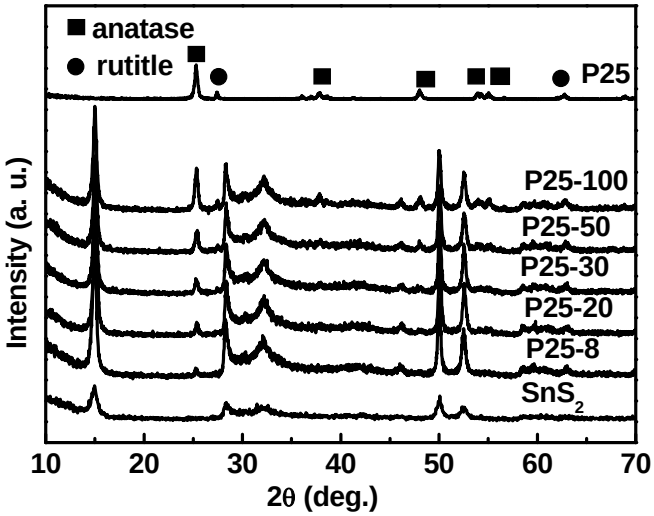

Fig. 1. XRD patterns of SnS_2, (P25-8) ~ (P25-100) and TiO_2 derived from the hydrothermal reaction

Fig. 2 (a)–(f) show the TEM images of the as-synthesized (P25-8) ~ (P25-100) and SnS_2 nanoflakes, which exhibit an anisotropic lamellar morphology. The origin for the formation of flake-like morphology maybe strongly related to the intrinsic anisotropic nature of hexagonal phase SnS_2, which adopts a CdI_2-related crystal structure.

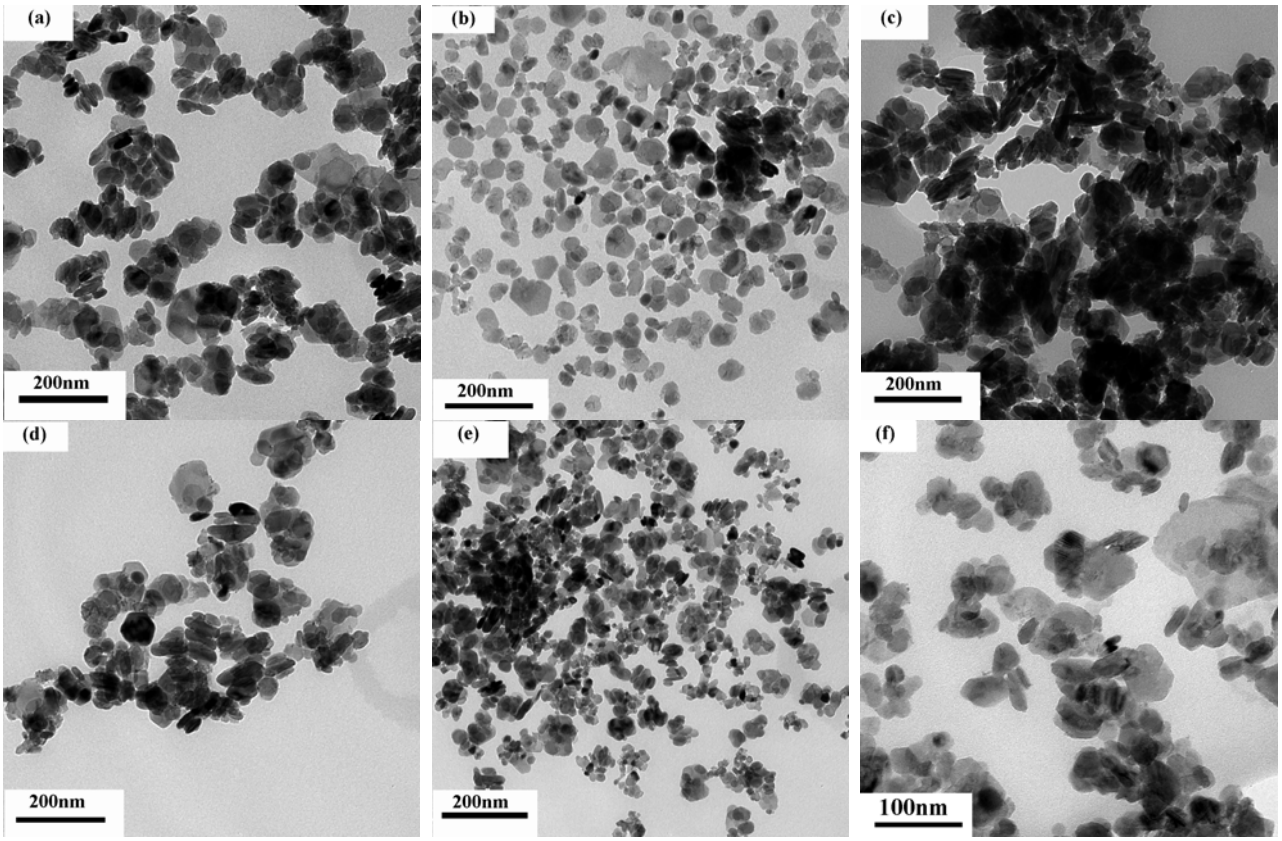

Fig. 2. The TEM images of the as-synthesized composition (P25-8) ~ (P25-100) and SnS_2 nanoflakes

The particle sizes of SnS_2, (P25-8) ~ (P25-100) and P25 TiO_2 observed by TEM are 23 - 42 nm, 19 - 34 nm, 32 - 53 nm, 39 – 57 nm, 27- 47 nm, 18 - 35 nm, respectively. Although there is defference between the particle sizes derived from TEM and Scherrer formula, the size evolving trends derived from the two kinds of methods are consistent with each other, the difference in the particle sizes derived from TEM and Scherrer formula may be due to the aggregation and shape effects of the nanoparticles.

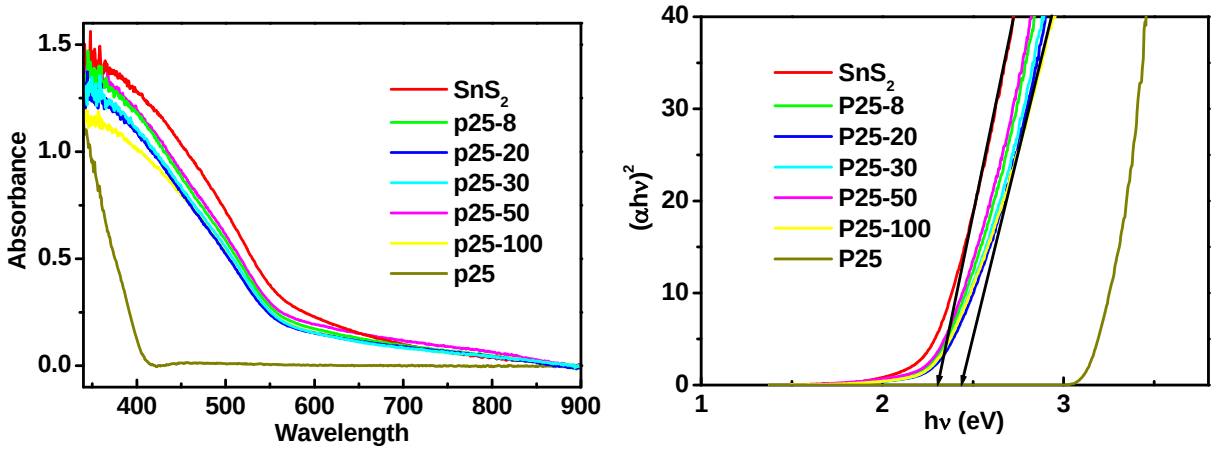

Fig. 3. the plots of $(a\ h\nu)^2$ against (hν) for the SnS_2, (P25-8) ~ (P25-100) and TiO_2

Fig. 3 shows the UV–vis diffuse reflectance spectra of the as-synthesized SnS_2, (P25-8) ~ (P25-100) and P25 TiO_2 nanoflakes. It can be seen that all the SnS_2 and SnS_2/TiO_2 products display optical absorption capabilities nearly in the entire visible light spectrum, which is commonly defined in the wavelength range of 400–700nm. The broad spectrum response suggests that the as-synthesized SnS_2 based nanoflakes should be excellent visible light-responsive photocatalysts for degrading organic pollutants. The optical bandgaps are deter-mined based on the theory of optical absorption for direct bandgap semiconductors[7, 8]:

$$\alpha h\nu = A\ (h\nu - E_g)^n$$

Where A is a constant, α is the absorption coefficient, hν is the discrete photon energy, and E_g is the optical band gap. The value of n for direct allowed transition is 1/2. The curves of $(\alpha h\nu)^2$ vs (hν) for the as-synthesized SnS_2 and SnS_2/TiO_2 nanoflakes are plotted in Fig. 3. By extrapolating the straight line portion of the plots of $(\alpha h\nu)^2$ vs (hν) to α = 0, the E_g values of SnS_2, (P25-8) ~ (P25-100) and P25 TiO_2 are estimated to be 2.24 eV, 2.32~2.41 eV, 3.5 eV.

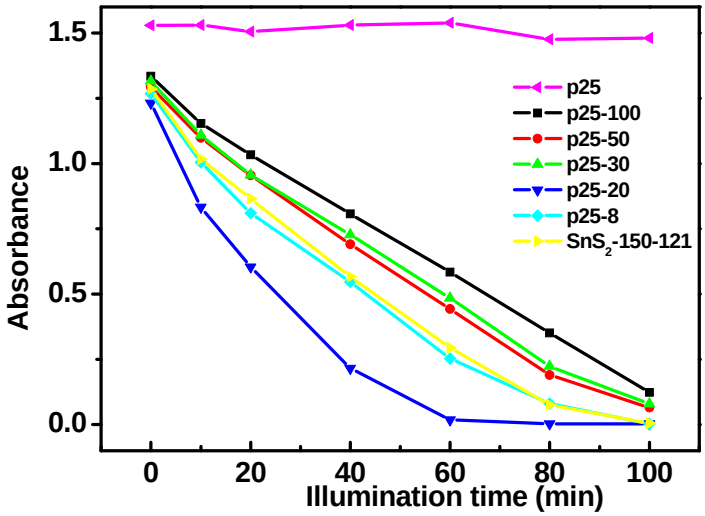

Fig. 4. Degradative evolution of MO in presence of as-synthesized photocatalysts under the visible light irradiation

Fig. 4 shows the degradative evolution of MO in presence of SnS_2, (P25-8) ~ (P25-100) and P25 TiO_2 under the visible light irradiation. It revealed that the degradative ratios of MO use P25-8 and P25-20 photocatalysts were faster than SnS_2, and the degradative ratios of MO used the rest composition photocatalysts were lower than SnS_2.

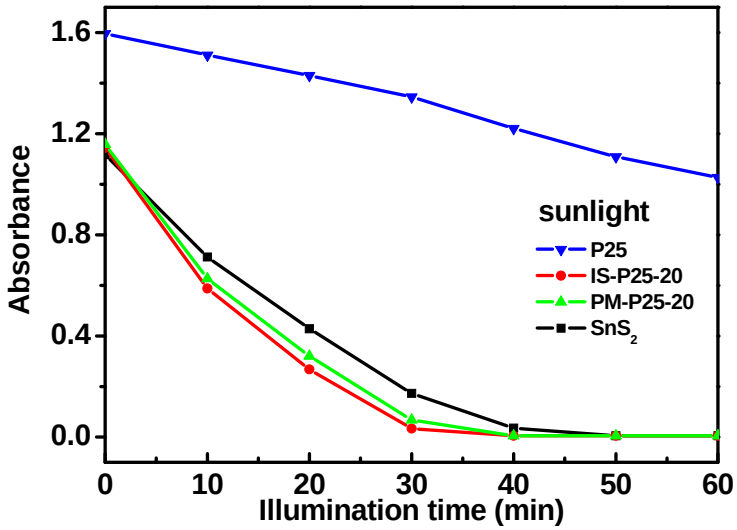

Fig. 5. Degradative evolution of MO in presence of SnS_2, P25-20, PM-P25-20 and P25 TiO_2 under the sunlight irradiation

Fig. 5 shows the degradative evolution of MO in presence of SnS_2, P25-20 and P25 TiO_2 under the visible-light irradiation. We can see that the degradative rates of MO are faster under the real sunlight irradiation than under the visible light. The fastest sample is P25-20. In addition, the physical mixtion sample according to molar ratios of Ti:Sn is 0.2 from the chemical solution, in order to facilitate the description, we abbreviated as PM-P25-20, its degradative rate is fast than the SnS_2 but lower than P25-20. It was assumed that the much superior photocatalytic performance of P25-20 was chiefly ascribed to the matching band potentials of SnS_2 and P25 TiO_2, and the efficient charge transfer and separation at their tightly integrated interface. The aforesaid photocatalytic results indicated that P25

TiO_2-20 should be a more promising photocatalyst in utilization of visible light and solar energy for degrading aqueous azo dyes.

4. Conclusions

Through the photocatalytic experiments using aqueous MO as a probe, the following results were obtained: (1) SnS_2 based composite photocatalysts with high visible light photocatalytic activity were synthesized via the hydrothermal reaction (2) under both the visible light ($\lambda > 420$ nm) and natural sunlight irradiations, P25 TiO_2 demonstrated higher photocatalytic efficiencies than the same amounts of SnS_2 and PM-P25-20 in the complete decolorization of 20mg/L MO aqueous solutions, and all the SnS_2-based photocatalysts were much more efficient than P25 TiO_2; (3) the matching band potentials of SnS_2 and P25 TiO_2 and the efficient charge transfer and separation at their tightly integrated interface. The aforesaid photocatalytic results indicated that P25-20 should be a more promising photocatalyst in utilization of visible light and solar energy for degrading aqueous azo dyes.

Acknowledgements

This work was financially supported by Natural Science Fund for Colleges and Universities in Jiangsu Province (14KJB430022), the Cultivating project of Xuzhou Institute of Technology (No. XKY2014103), and Innovative entrepreneurial training program of college student in Jiangsu province (xcx2015043).

References

[1] C. Yang, W. Wang and Z. Shan: J. Solid State Chem. Vol. 182 (2009) , p. 807-812.

[2] X. Li, J. Zhu and H. Li: Appl. Catal. B vol. 123–124 (2012) , p. 174-181.

[3] Y.C. Zhang, Z.N. Du and K.W. Li: ACS Appl. Mater. Interfaces vol. 3 (2011), p. 1528-1537.

[4] Y.C. Zhang, Z.N. Du and S.Y. Li: Appl. Catal. B vol. 95 (2010), p. 153-159.

[5] R. Lucena, F. Fresno, F.C. Conesa: Appl. Catal. A vol. 415-416 (2012) , p. 111-117.

[6] Y.C. Zhang, J. Li and H.Y. Xu: Appl. Catal. B vol. 123-124 (2012), p. 18-26.

[7] R. Gherbi, N. Nasrallah, A. Amrane, R. Maachi, M. Trari: J. Hazard. Mater. Vol. 186 (2011) , p. 1124-1130.

[8] N. Nasrallah, M. Kebir, Z. Koudri, M. Trari, J. Hazard. Mater. Vol. 185 (2011) , p. 1398-1404.

